Dietary supplementation with nacre reduces cortical bone loss in aged female mice

Dung Kim Nguyen, Arnaud Vanden-Bossche, Norbert Laroche, Mireille Thomas, Marie-Thérèse Linossier, Sylvie Peyroche, Delphine Farlay, Hélène Follet, Patrice Laquerrière, Marie-Hélène Lafage-Proust, et al.

Dietary supplementation with nacre reduces cortical bone loss in aged female mice

Dung Kim Nguyen [a,*,] Arnaud Vanden-Bossche [a], Norbert Laroche [a], Mireille Thomas [a], Marie-Therese Linossier [a], Sylvie Peyroche [a], Delphine Farlay [b], Helene Follet [b], Patrice Laquerriere [c,d], Marie-Helene Lafage-Proust [a,e], Thierry Thomas [a,e], Laurence Vico [a], Hubert Marotte [a,e], Marthe Rousseau a,f

[a] Université Jean Monnet Saint-Etienne, INSERM, Mines Saint Etienne, SAINBIOSE U1059, F-42023 Saint-Etienne, France

[b] INSERM, LYOS UMR 1033, Université Claude Bernard Lyon 1, 69008 Lyon, France

[c] Université de Strasbourg, Strasbourg, France

[d] CNRS, Institut Pluridisciplinaire Hubert Curien UMR 7178, Strasbourg, France

[e] Université Jean Monnet Saint-Etienne, Department of Rheumatology, CHU Saint-Etienne, INSERM, Mines Saint Etienne, SAINBIOSE U1059, F-42023, F-42055 Saint-Etienne, France

[f] UMR5510 MATEIS, CNRS, Lyon University, INSA-Lyon, Lyon, France

Abstract

Aging is associated with detrimental bone loss leading to fragility fractures in both men and women. Notably, a majority of bone loss with aging is cortical, as well as a large number of fractures are non-vertebral and at the non-hip sites. Nacre is a product of mollusks composed of calcium carbonate embedded in organic components. As our previous study demonstrated the protective effect of nacre supplementation on trabecular bone loss in ovariectomized rats, we sought to evaluate the effect of dietary nacre on bone loss related to aging in female mice which do not suffer true menopause as observed in women. The current study compared the effect of a 90-day long nacre-supplemented diet to that of Standard or $CaCO_3$ diets on both bone mass and strength in 16-month-old C57BL/6 female mice. Multiple approaches were performed to assess the microarchitecture and mechanical properties of long bones, analyze trabecular histomorphometry, and measure bone cell-related gene expressions, and bone turnover markers. In the cortex, dietary nacre improved cortical bone strength in line with lower expression levels of genes reflecting osteoclasts activity compared to Standard or $CaCO_3$ diets ($p<0.05$). In the trabeculae, nacre-fed mice were characterized by a bone remodeling process more active than the other groups as shown by greater histomorphometric parameters and osteoblast-related gene expressions ($p<0.05$). But these differences were not exhibited at the level of the trabecular microarchitecture at this age. Collectively, these data suggest that dietary nacre should be a potential candidate for reducing aging-associated cortical bone loss in the elderly.

Keywords: Osteoporosis, Aging, Bone, Nacre, Animal Experimentation

Introduction

Fracture due to bone fragility imposes a significant healthcare burden on society, in which a substantial proportion is on people under 70 years or non-osteoporosis (Mai et al., 2019). For such reason, prevention targeting the aging population is likely to be more effective in reducing the healthcare burden of fractures than treating people with diagnosed osteoporosis or previous fracture alone (LeBoff et al., 2022). Age-related loss of bone mass and strength is an invariable feature of the skeleton, affecting women and men alike. Although sex and aging are key clinical risk factors for bone fragility, aging is attributable to bone loss more considerably than estrogen deficiency in women (Almeida et al., 2017). Over the age of 65, most bone loss is cortical (Almeida et al., 2017), and notably, non-vertebral, non-hip fractures are approximately 5 times more common than the spine and hip fractures combined (Watts, 2014). Indeed, preventive strategies focused on cortical bone loss (such as appropriate calcium and vitamin D intakes, exercise, and avoiding falls), if provided at earlier stages, should reduce the risk of fractures.

Current osteoporotic therapies include antiresorptive and anabolic treatment which eventually cause side effects on several organs peri- and post-period of treatment (LeBoff et al., 2022). To date, very few molecules with dual effects on both osteoclasts and osteoblasts have been found (Wang et al., 2020). Therefore, identifying new anti-osteoporotic candidates, that combined with antiresorptive, anabolic mechanisms, and low toxicity, remains an interesting development in osteoporosis prevention and treatment.

Diet is probably one of the most modifiable factors for influencing health and the effects of aging (Campisi et al., 2019). For bone health, the development of herbal supplements is emerging in the nutrition field (Canivenc-Lavier and Bennetau-Pelissero, 2023). While many drugs of marine origin have been explored for their therapeutic properties in various chronic diseases, such as cancer or chronic inflammation (Malve, 2016), there have been few studies using products from aquatic organisms to target bone health. Nacre is a part of the exoskeleton of mollusks composed of calcium carbonate ($CaCO_3$) embedded in an organic matrix (Song et al., 2019), whose beneficial effects on bone cells have been documented through *in vitro* works (Lin et al., 2020, Li et al., 2018). Recent preclinical investigations suggested that nacre should be a candidate for therapeutic use in osteoporosis (Nguyen et al., 2022, Li et al., 2018). However, these studies only focused on bone loss due to estrogen deficiency in young animals. Therefore, we sought it was of high interest to evaluate the effect of nacre on bone loss related to aging, regardless of deficient sexual hormone state as done in previous studies.

Here, we present the result of a study evaluating the effect of nacre supplementation on bone health in aged female mice through the following approaches: (i) assessing the microarchitecture of both cortical and trabecular compartments, as well as cortical bone strength; (ii) measuring serum bone

turnover markers levels at various time points during the study; (iii) performing quantitative trabecular histomorphometry and gene expression in femur samples.

Materials and Methods

Animals

Sixteen-month-old female C57BL/6 mice (body weight: 29.5 ± 4.2 g mean ± SD) were used in this study (Fig. S1). These mice were weaned after 1 month of birth, and female littermates were selected and kept under same environmental conditions to match ideal controls with respect to age over the course of this study (Brayton et al., 2012). Also, these mice did not undergo pregnancy before. Mice were housed in cages (n=4/cage) with ad libitum access to water and food under standard laboratory conditions (22°C ± 1°C, 50% to 80% relative humidity, 12-hour light/dark cycle). Before weaning, these mice were fed with growing diet (SAFE A03, Augy, France), then a transition period to maintenance diet (SAFE R05-10, Augy, France) was done. The animals received quality attention and care by qualified personnel, both during and outside of procedures, to ensure optimal well-being throughout the study (Approval Number: APAFIS#25560-2020052510545037 v3).

Study design

Mice were divided into 3 groups and were fed with different diets: either Standard food (SAFE R05-10, Augy, France containing 8.5 mg calcium/g food under the form of $CaCO_3$, Standard group) or experimental foods. In these two later, Standard food was enriched with either 0.25% $CaCO_3$ (Reference C4830, Sigma-Aldrich, MO, USA) ($CaCO_3$ group) or 0.25% nacre powder from *Pinctada maxima* (Nacre group). The calcium dose was 9.5 mg/g food in both experimental diets (see Table S1). Nacre powder was provided by Stansea which has the know-how to reduce nacre into powder in a way that preserves the active organic compounds contained in nacre (i.e., proteins, peptides, lipids).

During the study period (i.e., 90 days), mice were weighed every 2 weeks and blood was collected at days 0, 45, and 90. Injections of tetracycline (Sigma T3383, St Quentin Fallavier, France, 25 mg/kg body weight) were done 8 and 3 days before killing. The final age of mice was 19 months. Mice were sedated with 4% isoflurane and then decapitated. The tissue collection is described below.

Dual-energy-ray absorptiometry (DXA) and microcomputed tomography (µCT)

Longitudinal DXA and µCT

Mice underwent *in vivo* DXA (Piximus, Lunar Corporation, Madison, WI) and *in vivo* µCT (Scanco VivaCT 40, Bruttisellen, Switzerland) at both the baseline and final time point of the study (See details in Supplementary Information section 1). The nomenclature used conforms to the recommendations of the American Society for Bone and Mineral Research (Bouxsein et al., 2010). Trabecular parameters: bone volume fraction (BV/TV, %), connectivity density (Conn.D, $1/mm^3$), trabecular number (Tb.N, 1/mm), trabecular thickness (Tb.Th, mm), trabecular separation (Tb.Sp, mm), structure model index

(SMI) and bone mineral density (BMD, mg/cm^3). Cortical parameters: cortical area (Ct.Ar, mm²), cortical thickness (Ct.Th, mm), marrow area (Ma.Ar, mm²), tissue mineral density (TMD, mg/cm^3) and cortical porosity (Ct.Po, %).

Cross-sectional µCT

The right femora with surrounding soft tissue were stored at -20°C after dissection. The soft tissue was removed before imaging the whole bone with a Skyscan 1176 scanner (Bruker-microCT, Kontich, Belgium). Images were acquired using the following settings: 9 µm isotropic voxel, 0.5 mm aluminum filter, 50 kV voltage, 500µA current, 1000 ms exposure time, rotation 0.6 degrees and frame averaging = 1. 3D images were reconstructed with the SkyScan software program NRecon (Bruker, version 1.7.4.6), with 20% beam hardening correction, at Gaussian smoothing = 1 (sigma = 0.5, and support = 3). Bone mineral density (BMD) calibration 2mm - diameter phantoms in pairs with calcium hydroxyapatite concentration of 0.25 and 0.75 g/cm^3 were acquired with attenuation coefficient (AC), which were 0.048319 and 0.022053, respectively. The BMD was calculated as follows: BMD = (AC – 0.061452) / -0.052532 g/cm^3. The images then were analyzed by CT-Analyser (Bruker, version 1.20.3.0), DataViewer (Bruker, version 1.5.6.2), and CT-Vox (Bruker, version 3.3.1).

For trabecular bone microstructure analysis, the volume of interest (VOI) was determined by identifying the distal end of the femur and calculating 14.5% of the femur length towards the femoral head, where we then analyzed a VOI of 1.8 mm (200 slices). The global greyscale threshold technique (corresponding BMD) was applied for analysis at 50 (0.68 g/cm^3).

Cortical bone was evaluated at two different sites. The authors counted 0.45 mm (50 slices) from the end of the trabecular VOI, then evaluated the first cortical 0.45 mm-high VOI (50 slices). In the next step, the authors measured a second 0.54 mm high cortical VOI (60 slices) located at 56% of the femur length, starting from the distal end of the femur towards the middle of the femur. Both cortical VOIs were evaluated with the threshold value of 64 (0.55 g/cm^3).

Mechanical testing of cortical bone

Cortical bone strength was assessed by three-point bending performed on the same right femora. Mechanical properties of the femoral midshaft were acquired as previously described (Schriefer et al., 2005). Before mechanical testing, the right femora were wrapped in cotton gauze moistened in phosphate-buffered saline at room temperature, which prevented sample dehydration during scanning. Measurements were performed with an ElectroForce 5500 test instrument (TA Instrument, New Castle, CA). The femur was positioned horizontally, with its posterior surface on the lower support of the bending apparatus, centered on the support, and pressing force was applied vertically to the bone midshaft. The lower supports were 8 mm apart. Each bone was tested with a preload (20 sinusoidal cycles of 0.5 N), then a bending load was applied at 0.05mm/s until failure with a 45 N load cell. The

load-displacement curve was acquired using the WinTest7 software and Breakage Energy (N.mm), maximal load, Fmax (N), and Stiffness (N/mm) were quantified.

Bone histomorphometry

The right femora of another batch of mice were harvested during dissection and fixed in 10% neutral-buffered formalin for 72 hours, then in 70% ethanol for 14 days at 4°C. The distal one-third of the femur was cut, then embedded undecalcified in methyl methacrylate following dehydration in 100% ethanol. Nine µm-thick frontal sections for staining and 12 µm - thick sections for dynamic analysis were cut using a microtome (SM2500; Leica Biosystems Nussloch GmbH, Germany) and mounted on slides. The 9 µm – thick sections were stained with Goldner's trichrome and tartrate-resistant acid phosphatase (TRAcP) to assess the microstructure and visualize osteoclasts, respectively. Unstained 12 µm – thick sections were analysed for the dynamic indices of bone formation based on tetracycline labeling. The description of histomorphometric parameters, and devices are provided in Supplementary Information section 1. The name of all histomorphometric parameters are given according to the histomorphometry nomenclature published by the American Society for Bone and Mineral Research Histomorphometry Nomenclature Committee (Dempster et al., 2013).

Biochemical markers of bone turnover

Mice fasted overnight before blood collection, which was performed in the morning to minimize intra-individual variation due to circadian rhythms. Blood was collected into 0.6 ml microcentrifuge tubes by retro-orbital bleeding at day D0, D45, and decapitation (D90). Blood was centrifuged at 13,000 g for 2 minutes at room temperature to collect serum, and stored in protein–low bind tubes at -80°C until measurement.

C-terminal cross-linking telopeptide of type I collagen (CTX), N-terminal propeptide of procollagen type I (P1NP), Osteocalcin, parathyroid hormone (PTH), fibroblast growth factor 23 (FGF23) were measured using mouse RatLaps CTX-I EIA kit (Immunodiagnostic systems, Boldon, UK), mouse/rat P1NP EIA kit (Immunodiagnostic systems, Boldon, UK), mouse Osteocalcin EIA kit (Immunotopics, San Clemente, CA, USA), mouse PTH 1-84 ELISA kit, and mouse/rat FGF23 Intact ELISA kit (Immunotopics, San Clemente, CA), respectively. Also, serum calcium and inorganic phosphate levels were measured with colorimetric assays (Biolabo SAS, Maizy, France).

qRT-PCR analysis

The bone marrow and the cortical compartment of the left femur were separated by flushing with a syringe and then immediately frozen in liquid nitrogen. Total RNA was extracted with TRI Reagent® (Sigma, St Louis, MO) and then purified with a Qiagen pure tissue kit (RNeasy Plus Mini Kit, Qiagen, Valencia, CA). The RNA quality was assessed with an Experion automated electrophoresis station (BioRad, Hercules, CA), followed by Ribogreen assay (Quant-iT RiboGreen RNA assay kit, Invitrogen, Life Technologies, Eugene, OR) for accurate RNA quantification. Total RNA reverse

transcription was performed with an iScript cDNA synthesis kit (BioRad). Quantitative real-time (qRT) polymerase chain reaction (PCR) was conducted on a CFX96 RealTime System (BioRad) with LightCycler FastStart DNA Master plus SYBRgreen I kit (Roche Diagnostics, Basel, Switzerland). The mRNA expression levels were normalized on the *Hprt1* housekeeping gene using the ΔCt method (Livak and Schmittgen, 2001). Primer sequences are shown in Table S2.

Statistical method

Biomechanical parameters for each group were individually adjusted to body weight, as previously described by Jepsen et al. (Jepsen et al., 2015) using a linear regression method with the following formula:

$$Trait(adj)_i = Trait(unadj)_i - slope\ (trait\ vs\ body\ weight) \times (body\ weight_i - mean\ body\ weight)$$

The adjusted trait was calculated for each mouse (i) in each group. The slope of the linear regression between the trait and body weight was calculated separately for each group. The mean body weight was calculated as the average of the three group means (Standard, $CaCO_3$, and Nacre groups) (Jepsen et al., 2015). Both unadjusted and adjusted data sets were then used for further statistical analysis.

The analyses were using the R Statistical Environment, version 4.1.3 (R Foundation for Statistical Computing). Data were checked for normality using Quantile-Quantile plots and all variables were tested for skewness and kurtosis.

For prospective experiments, (i) comparisons between groups in DXA and μCT (Scanco) experiments were performed using analysis of covariance (ANCOVA) general linear models using values at baseline as covariable (Vickers, 2001). The outcomes of statistic test $F(df_{between}, df_{within})$, p-values of the group effect whilst adjusting for baseline, and effect size (generalized eta squared, η_g^2) were showed in figures. Tukey's Honest Significant Difference (HSD) posthoc test was then performed to report 95% confidence intervals (CI); (ii) Biochemical marker levels were analyzed by two-way repeated-measures analysis of variance (ANOVA) to determine if there were group effect (between-subjects factor), time effect (within-subjects factor), and interaction between them. After ANOVA, Tukey's HSD post-hoc test was used for multiple comparisons between groups and between the value at the time point versus that at a previous time point in each group (Garcia-Valencia et al., 2018).

For cross-sectional experiments, ANOVA was conducted followed by Tukey's HSD post-hoc test. If data did not follow a normal distribution, and to determine confidence intervals (Henderson, 2005), the Bootstrapped ANOVA analysis was performed with the "ANOVA.boot" function, followed by pairwise comparisons with the "wild.boot" function included in the "lmboot" package to present 95% CI and p-values. Data were randomly resampled 1000 times because, given the characteristics of the data, that number of replicates maximized accuracy in the prediction of mean differences, standard error of mean difference, and power (Pattengale et al., 2010). The bias–corrected and accelerated

confidence interval was used (Efron, 1987). p-values were followed by Benjamini-Hochberg procedure for multiple comparisons.

A nominal p-value of 0.05 was considered statistical significance. Besides p-values, 95% confidence intervals (95% CI) are reported in the representation of evidence of effect (Nguyen, 2020). Data visualization was performed with the ggplot2 package.

Results

Changes in body weight and composition

A significant decline in body weight was observed over time in mice of 3 groups, but this decline was attenuated at least 2-fold in both $CaCO_3$ and Nacre groups as compared to Standard (Fig. S2 A-C). No decrease in total body BMD or BMC was observed over the 90 days after accounting for baseline values (Table S3). Both Standard and $CaCO_3$ groups showed a non-significant decrease of lean mass, while a regular increase of lean mass was observed in the Nacre group. Also, the Standard-fed mice lose about 2-fold of fat mass (p=0.02) over the 90-day period, but this fat mass decrease was not reach to significant sign in both $CaCO_3$ and Nacre groups. (Fig. S2 D). However, any differences of body compositions were observed between group after accounting to baseline values.

µCT analysis of the tibia and femur

Longitudinal µCT analysis of the tibia is presented in Table S4 and visualized in Fig. 1. The trabecular bone volume in the proximal metaphysis did not change significantly in Standard and $CaCO_3$ groups, while only Nacre group showed a 68% increase in BV/TV (p=0.05) over 90 days. But the difference between groups was not statistically significant after accounting to baseline values. Nacre-fed mice exhibited an increase of 5-fold in baseline-adjusted Conn.D compared to the $CaCO_3$ group (95% CI, 0.96 to 26.63, p=0.03) (Fig. 1A-C).

In the tibial midshaft (Fig. 1D-F), the magnitude of the response of cortical bone to dietary interventions differed among the 3 groups for Ma.Ar. The Standard group exhibited an increase of 9% in Ma.Ar respective to baseline (p=0.02). The $CaCO_3$-fed mice showed the same trend to Standard group but this change did not reach to significance. In contrast, the age-related loss of tibial cortical bone differently manifested in the Nacre group, which displayed a 6% decrease in Ma.Ar, in line with a 2% increase in TMD. At the end of the study, baseline-adjusted Ma.Ar was 12% lower (95%CI, -0.16 to -0.02; p=0.02) in the Nacre group than in the Standard group, while TMD was 3.7% higher on average (95%CI, -2.9 to 93.9; p=0.07).

Complementary to the longitudinal µCT analysis with the Scanco VivaCT40 scanner, we next sought to identify differences in femur microarchitecture between groups using a higher resolution of 9µm voxel size (Skyscan scanner, Fig. 2A) allowing for more reliable evaluation of cortical parameters. Representative µCT coronal images of the entire femur and 3-dimensional traversal images of the

femur diaphysis are shown in Fig. 2 B-D. At the distal femur, although the number of trabeculae was decreased in both $CaCO_3$ and Nacre groups as compared to Standard group ($p=0.05$), no significant difference was detected for the other parameters of trabecular bone (Fig. 2 E-H).

As expected, the Ct.Th of cortex was greater at the midshaft than at the distal metaphysis (site effect, $p<0.0001$, Fig. 2 I). A significant interaction between group and site indicated a differential response of the two sites to dietary interventions ($p=0.03$). Both $CaCO_3$ and Nacre groups had significantly higher Ct.Th than Standard group at the distal metaphysis ($p<0.01$), while no effect was observed at the midshaft. The dietary interventions induced significant differences in Ct.Po regardless of the bone sites (group effect, $p<0.0001$). At both sites, the Nacre group showed a 2.5-fold lower Ct.Po compared to $CaCO_3$ group ($p<0.001$), while Ct.Po of $CaCO_3$ group was higher than that Standard ($p<0.001$) ((Fig. 2 K).

Taken together, high-resolution µCT findings indicate that dietary nacre counteracted the age-related cortical porosity development in the femur. Ct.Th was only improved at the distal metaphysis under both Nacre and $CaCO_3$ diets.

Biomechanical three-point bending test of the whole femur

The femur mechanical properties were next evaluated by using three-point bending (Table 1, Fig. 3). To avoid misleading in interpretation of effect of dietary interventions, the mechanical parameters were adjusted by eliminating the partial impact of body weight that was differentially observed between mice at the end. Figure 3A shows the Load / Displacement curves of the heaviest and lightest mouse from each group. The mice fed with nacre displayed higher biomechanical parameters, regardless of body weight.

Raw data on Breakage Energy show that the Nacre group exhibited significantly higher biomechanical resistance than both the $CaCO_3$ group (+34%; 95%CI, 0.32 to 2.31; $p<0.001$), and the Standard group (+31%; 95%CI, 0.16 to 2.45; $p=0.008$) which did not differ from each other (Fig. 3 B). These differences held after adjustment for body weight (Fig. 3 E), with differences in the slope of Breakage Energy over body weight regression (Fig. 3 H-I).

Similarly, Nacre mice showed the highest Fmax among the 3 groups, which persisted even after adjusting for body weight (Fig.3 C and F), as illustrated in graphs of Fmax over body weight (Fig. S3 A).

Stiffness did not differ significantly between groups (Fig. 3 D and G). The stiffness versus body weight regressions shows the overlap in Stiffness values or no difference in slope between pairwise comparisons (Fig. S3 B).

Histomorphometric analysis of trabecular bone in the distal femoral metaphysis

Figure S4 illustrates trabecular bone amounts, and cellular parameters in the three groups. In agreement with µCT data, no difference in trabecular bone volume (BV/TV) and thickness (Tb.Th) was observed in the femur proximal metaphysis (data not shown). The osteoclasts-related parameters were higher in Nacre group (Fig. 4 A-C) as compared to Standard and $CaCO_3$ groups. Osteoclasts were more abundant in the Nacre group than in both the Standard and $CaCO_3$ groups ($p<0.001$). Osteoclast surface was more extended in the Nacre group than in Standard (+1.6 folds; 95%CI, -0.18 to 2.26; p=0.06), and in $CaCO_3$ group (+1.8 folds; 95%CI, 0.08 to 2.32; p=0.03). No difference was observed between the Standard and $CaCO_3$ groups. Interestingly, with regard to bone formation parameters, MAR, and BFR values were higher in Nacre than in $CaCO_3$ and Standard group ($p<0.05$), while no difference was observed between 2 later groups (Fig. 4 D-F).

Effect of dietary interventions on gene expression of bone cells

In line with the increase in trabecular bone formation parameters, the authors indicated a higher *Bmp2* expression in the marrow compartment of the Nacre group than that of Standard (+2 folds; 95%CI, 0.23 to 1.72; p=0.008) and $CaCO_3$ group (+1.8 folds; 95%CI, 0.26 to 1.68; p=0.002). *Runx2* expression was also higher in the Nacre group than in $CaCO_3$ group (+3 folds; 95%CI, 0.02 to 0.39; p=0.03) (Fig. 5A). No difference was detected between $CaCO_3$ and Standard groups for these two genes.

RNA assayed in the marrow-free femur samples reflects the activity of a heterogeneous cell populations including mature osteoblasts and osteoclasts lining the periosteal and endosteal bone surfaces, as well as osteocytes (Fig. 5 B). The expression of *Sost*, coding for sclerostin, an inhibitor of bone formation, was lower in nacre-fed mice than in the $CaCO_3$ group (-5.4 folds; 95%CI, -11.93 to -0.19; p=0.02), whereas inversely $CaCO_3$-fed mice showed a 7.7-fold higher expression as compared to the Standard group (95%CI, 1.16 to 12.30; p=0.03). The $CaCO_3$-fed mice exhibited the highest mRNA levels of osteoclast – related genes (*Acp5*, and *Cathepsin K*), whereas the lowest levels were observed in the Nacre group ($p<0.05$). Expression of *Spp1*, encoding osteopontin which is known as an anchor of osteoclasts to the bone surface, was significantly attenuated at least 4 folds in the Nacre group compared with the two other groups ($p<0.05$) (Fig. 5B).

Effect of dietary intervention on bone turnover markers

The changes of bone turnover markers were measured in serum (Fig.6 A-C). In all groups, a reduction with time was observed for osteocalcin and P1NP levels (time effect, $p<0.001$), while CTX levels remained stable over the 90-day period (time effect, $p>0.05$). No interaction between time and group was detected for these markers. However, P1NP and CTX levels were lower in $CaCO_3$ and Nacre mice as compared to Standard mice at day 90 ($p<0.05$).

Finally, the measurement of PTH levels was performed, a hormone that regulates calcium metabolism and is mainly driven by calcium serum levels, and of FGF23, a bone-derived phosphaturic hormone at

day 90. Total calcium, phosphate, and FGF23 levels did not differ between the 3 groups (Fig. 6 D-F). Lower PTH serum levels were observed in mice under either $CaCO_3$ or Nacre compared to Standard ($p<0.001$) (Fig. 6 G).

Discussion

The authors recently showed that supplementation with nacre counteracts the accelerated trabecular bone loss in ovariectomized rat model (Nguyen et al., 2022). Both aging and sex steroids deficiency cause osteoporosis, but their impact on the skeleton are mechanistically distinct and concurrently occur in the livings (Ucer et al., 2017, Farr et al., 2019). Importantly, aging contributes to the slow phase of bone loss in women that continues indefinitely (Almeida et al., 2017). During this phase, the cortical bone loss is dominant, and induces risk of fragility fractures. The present study addressed a small part of this complex pathophysiology to understand the effect of dietary nacre supplement on the sex steroid hormone-independent slow bone loss due to aging in aged female mice.

The standard-fed mice exhibited a decrease in body weight over time (Fig. S1). This reflects a decrease of food intake with aging through both peripheral and central mechanisms (Morley, 2001) and/ or of functional deficits of gastrointestinal system (i.e., impairments in gut microbiota, metabolite production) (Claesson et al., 2011). Calcium intake plays a pivotal role in weight management, especially in the attenuation of weight gain related to the role of intracellular Ca^{2+} in regulating lipid metabolism and triglyceride storage in both humans and mice (Zemel, 2005). To our knowledge, there has not been any previous work indicating the influence of dietary calcium on weight loss in aging. Despite of no statistically signs detected in changes of lean and fat mass due to a limited sample size of this experiment, an significant attenuation of body weight loss under $CaCO_3$ and Nacre diets suggests that dietary calcium may help mediating the normal activity of adipocytes, hence avoiding an imbalance in the lipid metabolism (Alomaim et al., 2019).

Aging is responsible for deterioration of both cortical and trabecular bone compartments (Ucer et al., 2017, Ling et al., 2021). Standard group exhibited a steady state for trabecular mass and microarchitecture at the tibial metaphysis between 16 and 19 months of age (Fig. 1 A-B, Table S4A). Moreover, the trabecular mass is so low at this age, so a lack of persuadable evidence for effect of nacre diet on trabecular bone can be expected in the terms of trabecular parameters. Meanwhile, marrow area continued to enlarged, and midshaft cortical TMD still decreased as observed in Standard group during 3 months (Fig. 1 D-E, Table S4B). These changes are caused by periosteal expansion and endocortical resorption (Shahnazari et al., 2012), leading to cortical thinning. Interestingly, nacre diet tended to both reduce marrow area enlargement and to improve cortical TMD over this 90-day period.

In contrast to what we observed in the estrogen deficiency-related bone loss in rats, we found no evidence of effect of either dietary $CaCO_3$ or nacre on trabecular bone at the femoral distal

metaphysis. The steady state of trabecular loss as discuss above through the longitudinal tibial microarchitecture would lead to be lower sensitivity to bone metabolism of trabecular bone in 19-month-old female mice. But the expansion of marrow area in the Standard group should indicate the cortical bone loss being continuing during the period of study. Indeed, the cortical thickness at the distal metaphysis responded to both $CaCO_3$ and nacre diets. Importantly, the Nacre group only had lower cortical porosity, as compared to the Standard group at both cortical sites. *De novo* intracortical remodeling that occurs with old age increases cortical porosity in mice (Piemontese et al., 2017), and supplementation with nacre could limit this process.

These cortical parameters could be put in perspective with bone strength evaluated by three-point bending test (Fig. 3 and S3). Breakage Energy and Maximum Load of the femur midshaft in mice receiving nacre diet were better than Standard group, while $CaCO_3$ had no significant effect. As both nacre and $CaCO_3$ diets rescued body weight loss and the heterogeneity in body weight among groups at baseline was observed, which subsequently may influence on cortical bone strength. We carefully adjusted the mechanical parameters for body weight. Interestingly, these differences were still remained after removing the impact of this confounder. A critical result demonstrates the effects of nacre on bone strength should be independent of body weight.

To further decipher the potential effect of dietary nacre on bone quality in the terms of bone cells and their activities, the histomorphometry and the gene expression at the distal femur were analyzed. Regarding trabecular bone loss with aging, Almeida et al. reported a decreased rate of remodeling as evidenced by decreased osteoblast and osteoclast numbers and decreased BFR in the trabecular vertebrae of female C57BL/6 mice between 8 and 31 months of age (Almeida et al., 2007). Also, previous histomorphometric analysis of the trabeculae at the distal femur from this mouse strain indicated a decrease in osteoblast surface and bone formation rate between 6 weeks and 24 months of age (Cao et al., 2005). These changes are associated with a decline of bone marrow-derived mesenchymal or osteoblast progenitor function with age (independent of sex steroid deficiency) in both human and rodent cells (Stenderup et al., 2003, Coipeau et al., 2009). Of note, the nacre-fed mice exhibited higher osteoclast-related parameters (i.e., number and active surfaces) and a higher bone formation rate as compared to Standard and $CaCO_3$ groups (Fig. 4) based on no difference of BV/TV between groups. Furthermore, osteoblast-related mRNAs expression was more abundant under nacre diet than two others (Fig. 5). These findings herein suggest that dietary nacre may limit the decline of bone cells due to aging.

Regarding cortical bone loss with aging, cortical expansion and porosity are generally associated with increased remodeling (Piemontese et al., 2017). The cortical expansion in aged C57BL/6 mice included the increased periosteal surface area that is likely reflecting increased bone formation, and increased endocortical surface, likely due to increased endocortical resorption (Shahnazari et al., 2012). The increased cortical porosity results from *de novo* intracortical remodeling by osteon-like

structures favoring resorption with advancing age (Piemontese et al., 2017). A significant decrease in cortical osteoclast-related mRNAs was shown in the Nacre group (Fig. 5). The combination of μCT and biomechanical findings suggest that nacre should protect cortical bone from the unbalance of cortical remodeling. These results are corroborated by the reduced cortical porosity observed in nacre-fed mice as compared to the two other groups. In contrast to nacre, $CaCO_3$ diet induced a higher cortical thickness than that of standard diet, and an increase of cortical porosity as compared to two other diets in the femur (Fig. 2 I-K), suggesting that supplementation with $CaCO_3$ would preserve the cortical thickness from unbalance of cortical expansion, but not intra-cortical remodeling related to porosity. These findings are associated with increased mRNA levels reflecting osteoclastic activity (Fig 5B). In general, the calcium fraction including in nacre may act on the cortex like $CaCO_3$ diet, other beneficial effects should be due to organic fraction.

Circulating bone turnover markers in aged mice reflect the dynamics of trabecular rather than cortical bone (Shahnazari et al., 2012). Products of cortical remodeling might be relatively low due to a lower blood supply of cortex than that of trabeculae (Shim, 1968). Both $CaCO_3$ and Nacre groups exhibited a decrease of CTX and P1NP as compared to the Standard group (Fig. 6 A-C). In fact, an increase in trabecular osteoblast-related mRNAs (Fig. 5) is consistent with the maintenance / strengthening of the trabecular remodeling in the Nacre group (Fig. 4). Such local markers in the marrow plasma might reflect more accurately the remodeling activity than circulating ones.

Finally, PTH is the major regulator of calcium homeostasis mainly via kidney and bone. The decreased ability of gut to absorb calcium with age limits the adaptation to low calcium intake and is thought to lead to secondary hyperparathyroidism (Ensrud et al., 2000, Nordin et al., 2004). This negative calcium balance stimulates PTH secretion, thus worsening age-related bone loss through increased osteoclastic resorption. Both $CaCO_3$ and Nacre groups exhibited significantly lower PTH levels than that of the Standard group with no difference between $CaCO_3$ and Nacre group, suggesting that any putative preservation of bone properties via reduction of secondary hyperparathyroidism was likely similar in the two former groups (Fig 6 G). The cellular and molecular findings support the hypothesis that this indirect effect is of limited importance. Bone strength was better under nacre than $CaCO_3$ diet (Fig. 3), suggesting that part of the nacre effects may be due to its organic fraction.

The present findings must be interpreted in the context of a number of potential limitations. An important strength of this study is that the first preclinical study investigated the effect of dietary nacre on bone loss due to aging in the duration of 90 days. The study performed several methods that are widely used in bone research to examine bone microarchitecture, strength and metabolism. Furthermore, by assessing longitudinal monitoring for some experiments, and by accounting for confounding body weight in the bone strength, we have addressed the overtime changes of bone microarchitecture, turnover, and the real effect of experimental diets on bone quality. However, the sample size in the study was relatively modest in some experiments (e.g., dynamic histomorphometry,

gene expression analysis), which limited our ability to provide solid evidences. To compensate for small sample sizes, we conducted the Bootstrap method to generate representative resampling population. Besides, this statistical method repairs the weaknesses of non-parametric methods (i.e., dichotomise p-values into significance and non-significance based on threshold of 0.05, and conclude a hypothesis testing) and helps to interpret the findings based on 95% confident interval. Importantly, we lack information of the cortical histomorphometric status and therefore the underlying mechanism by which nacre would act on cortical bone. Finally, food intake should be considered in further study to explain more precisely the changes in body weight and composition.

In conclusion, these data indicate that dietary nacre supplement reduce cortical bone loss evidenced by improving bone strength and attenuating cortical porosity formation through limiting the expression of gene related to osteoclasts and their activity. Besides, trabecular bone remodeling state is maintained under nacre diet instead of declining with aging, as done by indicators of both bone cells and bone dynamic formation. These data also suggest that the effect of supplementation with nacre could be of clinical relevance in osteoporosis in the elderly women and presumably to limit fragility fracture risk.

Acknowledgments

The authors thank the staff of PLEXAN (Platform for Animal Experimentation and Analysis, Medical School, Saint-Etienne, France) for supervision of animal care and Stansea for providing nacre powder. We gratefully thank Dr. Luc Malaval in our group for contributing to the present study with critical comments on the manuscript. We thank also our staff, Mrs. Stéphanie Mundweiler for checking the form of manuscript before submission.

Author contributions

Study design: MR, AVB. Study conduct: DKN, AVB, NL. Micro-CT: DKN, NL, HF. Bone biomechanical test: DKN, HF. Bone histomorphometry: DKN, NL. Blood biomarkers: DKN, MTL, SP. Gene expression: DKN, MT. Data analysis and visualization: DKN. Data interpretation: DKN, MHLP. Writing original draft: DKN. Revising manuscript content: DKN, MR, HF, MHLP, HM, TT, LV. Approving final version of manuscript: all authors.

Funding

This study was funded by the project NADO (ANR18 - CE18 – 0003 - 01) of the French National Research Agency (ANR).

Declarations

Conflict of interest

MR provides scientific consultation for Megabiopharma. TT reports receiving lecture fees from Amgen, Arrow, Biogen, BMS, Chugai, Galapagos, Grunenthal, Jansen, LCA, Lilly, MSD, Nordic, Novartis, Pfizer, Sanofi, Thuasne, Theramex, UCB and research grants or investigator's fees from Bone Therapeutics, UC. HM reports fees from Amgen, Arrow, Biogen, BMS, CellTrion, Chugai, Galapagos, Fresenius Kabi, Jansen, Lilly, MSD, Nodic, Novartis, Pfizer, Sanofi, and UCB. All other authors state that they have no conflicts of interest.

Ethical Approval

This study was carried out with the approval of the French Ministry of Research and Innovation (Approval Number: APAFIS#25560-2020052510545037 v3). Animal procedures were performed in an accredited animal facility (authorization no. C42180801) at the PLEXAN with the approval of the Animal Ethics Committee and by directive 2010/63/EU and the "Principles of Laboratory Animal Care" recommended by the National Society for Biomedical Research in France. No human studies were performed in the course of these experiments.

References

ALMEIDA, M., HAN, L., MARTIN-MILLAN, M., PLOTKIN, L. I., STEWART, S. A., ROBERSON, P. K., KOUSTENI, S., O'BRIEN, C. A., BELLIDO, T. & PARFITT, A. M. 2007. Skeletal involution by age-associated oxidative stress and its acceleration by loss of sex steroids. *Journal of Biological Chemistry,* 282**,** 27285-27297.

ALMEIDA, M., LAURENT, M. R., DUBOIS, V., CLAESSENS, F., O'BRIEN, C. A., BOUILLON, R., VANDERSCHUEREN, D. & MANOLAGAS, S. C. 2017. Estrogens and androgens in skeletal physiology and pathophysiology. *Physiological reviews,* 97**,** 135-187.

ALOMAIM, H., GRIFFIN, P., SWIST, E., PLOUFFE, L. J., VANDELOO, M., DEMONTY, I., KUMAR, A. & BERTINATO, J. 2019. Dietary calcium affects body composition and lipid metabolism in rats. *PloS one,* 14**,** e0210760.

BOUXSEIN, M. L., BOYD, S. K., CHRISTIANSEN, B. A., GULDBERG, R. E., JEPSEN, K. J. & MÜLLER, R. 2010. Guidelines for assessment of bone microstructure in rodents using micro–computed tomography. *Journal of bone and mineral research,* 25**,** 1468-1486.

BRAYTON, C., TREUTING, P. & WARD, J. 2012. Pathobiology of aging mice and GEM: background strains and experimental design. *Veterinary pathology,* 49**,** 85-105.

CAMPISI, J., KAPAHI, P., LITHGOW, G. J., MELOV, S., NEWMAN, J. C. & VERDIN, E. 2019. From discoveries in ageing research to therapeutics for healthy ageing. *Nature,* 571**,** 183-192.

CANIVENC-LAVIER, M.-C. & BENNETAU-PELISSERO, C. 2023. Phytoestrogens and Health Effects. *Nutrients,* 15**,** 317.

CAO, J. J., WRONSKI, T. J., IWANIEC, U., PHLEGER, L., KURIMOTO, P., BOUDIGNON, B. & HALLORAN, B. P. 2005. Aging increases stromal/osteoblastic cell-induced osteoclastogenesis and alters the osteoclast precursor pool in the mouse. *Journal of Bone and Mineral Research,* 20**,** 1659-1668.

CLAESSON, M. J., CUSACK, S., O'SULLIVAN, O., GREENE-DINIZ, R., DE WEERD, H., FLANNERY, E., MARCHESI, J. R., FALUSH, D., DINAN, T. & FITZGERALD, G. 2011. Composition, variability, and temporal stability of the intestinal microbiota of the elderly. *Proceedings of the National Academy of Sciences,* 108**,** 4586-4591.

COIPEAU, P., ROSSET, P., LANGONNÉ, A., GAILLARD, J., DELORME, B., RICO, A., DOMENECH, J., CHARBORD, P. & SENSEBÉ, L. 2009. Impaired differentiation potential of human trabecular bone mesenchymal stromal cells from elderly patients. *Cytotherapy,* 11**,** 584-594.

DEMPSTER, D. W., COMPSTON, J. E., DREZNER, M. K., GLORIEUX, F. H., KANIS, J. A., MALLUCHE, H., MEUNIER, P. J., OTT, S. M., RECKER, R. R. & PARFITT, A. M. 2013. Standardized nomenclature, symbols, and units for bone histomorphometry: a 2012 update of the report of the ASBMR Histomorphometry Nomenclature Committee. *Journal of bone and mineral research: the official journal of the American Society for Bone and Mineral Research,* 28**,** 2.

EFRON, B. 1987. Better bootstrap confidence intervals. *Journal of the American statistical Association,* 82**,** 171-185.

ENSRUD, K. E., DUONG, T., CAULEY, J. A., HEANEY, R. P., WOLF, R. L., HARRIS, E., CUMMINGS, S. R. & GROUP*, S. O. O. F. R. 2000. Low fractional calcium absorption increases the risk for hip fracture in women with low calcium intake. *Annals of internal medicine,* 132**,** 345-353.

FARR, J. N., ROWSEY, J. L., ECKHARDT, B. A., THICKE, B. S., FRASER, D. G., TCHKONIA, T., KIRKLAND, J. L., MONROE, D. G. & KHOSLA, S. 2019. Independent roles of estrogen deficiency and cellular senescence in the pathogenesis of osteoporosis: evidence in young adult mice and older humans. *Journal of Bone and Mineral Research,* 34**,** 1407-1418.

GARCIA-VALENCIA, O., GAROVIC, V. D., MILIC, N. M. & WINHAM, S. J. 2018. Why we need to report more than'Data were Analyzed by t-tests or ANOVA'. *eLife,* 7.

HENDERSON, A. R. 2005. The bootstrap: a technique for data-driven statistics. Using computer-intensive analyses to explore experimental data. *Clinica chimica acta,* 359**,** 1-26.

JEPSEN, K. J., SILVA, M. J., VASHISHTH, D., GUO, X. E. & VAN DER MEULEN, M. C. 2015. Establishing biomechanical mechanisms in mouse models: practical guidelines for systematically evaluating phenotypic changes in the diaphyses of long bones. *Journal of bone and mineral research,* 30**,** 951-966.

LEBOFF, M., GREENSPAN, S., INSOGNA, K., LEWIECKI, E., SAAG, K., SINGER, A. & SIRIS, E. 2022. The clinician's guide to prevention and treatment of osteoporosis. *Osteoporosis International***,** 1-54.

LI, L., WANG, P., HU, K., WANG, X., CAI, W., AI, C., LIU, S. & WANG, Z. 2018. PFMG1 promotes osteoblast differentiation and prevents osteoporotic bone loss. *The FASEB Journal,* 32**,** 838-849.

LIN, J.-B., WU, H., LIU, Y.-L., SHAW, P.-C. & LI, P.-B. 2020. N16 suppresses RANKL-mediated osteoclatogenesis by down-regulating RANK expression. *International journal of biological macromolecules,* 151**,** 1154-1162.

LING, W., KRAGER, K., RICHARDSON, K. K., WARREN, A. D., PONTE, F., AYKIN-BURNS, N., MANOLAGAS, S. C., ALMEIDA, M. & KIM, H.-N. 2021. Mitochondrial Sirt3 contributes to the bone loss caused by aging or estrogen deficiency. *JCI insight,* 6.

LIVAK, K. J. & SCHMITTGEN, T. D. 2001. Analysis of relative gene expression data using real-time quantitative PCR and the 2− ΔΔCT method. *methods,* 25**,** 402-408.

MAI, H. T., TRAN, T. S., HO-LE, T. P., CENTER, J. R., EISMAN, J. A. & NGUYEN, T. V. 2019. Two-thirds of all fractures are not attributable to osteoporosis and advancing age: implications for fracture prevention. *The Journal of Clinical Endocrinology & Metabolism,* 104**,** 3514-3520.

MALVE, H. 2016. Exploring the ocean for new drug developments: Marine pharmacology. *Journal of pharmacy & bioallied sciences,* 8**,** 83.

MORLEY, J. E. 2001. Decreased food intake with aging. *The Journals of Gerontology Series A: Biological Sciences and Medical Sciences,* 56**,** 81-88.

NGUYEN, D. K., LAROCHE, N., VANDEN-BOSSCHE, A., LINOSSIER, M. T., THOMAS, M., PEYROCHE, S., NORMAND, M., BERTACHE-DJENADI, Y., THOMAS, T. & MAROTTE, H. 2022. Protective Effect on Bone of Nacre Supplementation in Ovariectomized Rats. *JBMR plus,* 6**,** e10655.

NGUYEN, T. V. 2020. Common methodological issues and suggested solutions in bone research. *Osteoporosis and sarcopenia,* 6**,** 161-167.

NORDIN, B. C., NEED, A. G., MORRIS, H. A., O'LOUGHLIN, P. D. & HOROWITZ, M. 2004. Effect of age on calcium absorption in postmenopausal women. *The American journal of clinical nutrition,* 80**,** 998-1002.

PATTENGALE, N. D., ALIPOUR, M., BININDA-EMONDS, O. R., MORET, B. M. & STAMATAKIS, A. 2010. How many bootstrap replicates are necessary? *Journal of computational biology,* 17**,** 337-354.

PIEMONTESE, M., ALMEIDA, M., ROBLING, A. G., KIM, H.-N., XIONG, J., THOSTENSON, J. D., WEINSTEIN, R. S., MANOLAGAS, S. C., O'BRIEN, C. A. & JILKA, R. L. 2017. Old age causes de novo intracortical bone remodeling and porosity in mice. *JCI insight,* 2.

SCHRIEFER, J. L., ROBLING, A. G., WARDEN, S. J., FOURNIER, A. J., MASON, J. J. & TURNER, C. H. 2005. A comparison of mechanical properties derived from multiple skeletal sites in mice. *Journal of biomechanics,* 38**,** 467-475.

SHAHNAZARI, M., DWYER, D., CHU, V., ASUNCION, F., STOLINA, M., OMINSKY, M., KOSTENUIK, P. & HALLORAN, B. 2012. Bone turnover markers in peripheral blood and marrow plasma reflect trabecular bone loss but not endocortical expansion in aging mice. *Bone,* 50**,** 628-637.

SHIM, S. S. 1968. Physiology of blood circulation of bone. *JBJS,* 50**,** 812-824.

SONG, X., LIU, Z., WANG, L. & SONG, L. 2019. Recent advances of shell matrix proteins and cellular orchestration in marine molluscan shell biomineralization. *Frontiers in Marine Science,* 6**,** 41.

STENDERUP, K., JUSTESEN, J., CLAUSEN, C. & KASSEM, M. 2003. Aging is associated with decreased maximal life span and accelerated senescence of bone marrow stromal cells. *Bone,* 33**,** 919-926.

UCER, S., IYER, S., KIM, H. N., HAN, L., RUTLEN, C., ALLISON, K., THOSTENSON, J. D., DE CABO, R., JILKA, R. L. & O'BRIEN, C. 2017. The effects of aging and sex steroid deficiency on the murine skeleton are independent and mechanistically distinct. *Journal of Bone and Mineral Research,* 32**,** 560-574.

VICKERS, A. J. 2001. The use of percentage change from baseline as an outcome in a controlled trial is statistically inefficient: a simulation study. *BMC medical research methodology,* 1**,** 1-4.

WANG, Q., CHEN, D., JIN, H., YE, Z., WANG, C., CHEN, K., KUEK, V., XU, K., QIU, H. & CHEN, P. 2020. Hymenialdisine: a marine natural product that acts on both osteoblasts and osteoclasts and prevents estrogen-dependent bone loss in mice. *Journal of Bone and Mineral Research,* 35**,** 1582-1596.

WATTS, N. B. 2014. Insights from the global longitudinal study of osteoporosis in women (GLOW). *Nature Reviews Endocrinology,* 10**,** 412-422.

ZEMEL, M. B. 2005. The role of dairy foods in weight management. *Journal of the American College of Nutrition,* 24**,** 537S-546S.

Figures and figure captions

Fig. 1 Effect of nacre or calcium carbonate supplementation on changes of trabecular and cortical bone mass and microarchitecture between day 0 and day 90 at the tibia longitudinally assessed using µCT (Scanco). Representative 3-dimensional (3D) µCT images of the trabecular bone of the proximal metaphysis **(A)** and the cortical bone of the midshaft **(D)** from each group at day 0 and day 90. (**B, E**) The raw data show the mean, and 95% CIs. p-values in green: vs. Standard, in pink: vs. $CaCO_3$. * vs. Day 0, *p≤0.05. (**C, F**) Percent changes in BV/TV, Conn.D, Ma.Ar, and TMD in experimental diets-fed mice compared to Standard. Data represent the change of baseline-adjusted mean groups relative to Standard in % (Standard or $CaCO_3$: n=10, Nacre: n=6). Bone volume fraction (BV/TV), connectivity density (Conn.D), marrow area (Ma.Ar), tissue mineral density (TMD).

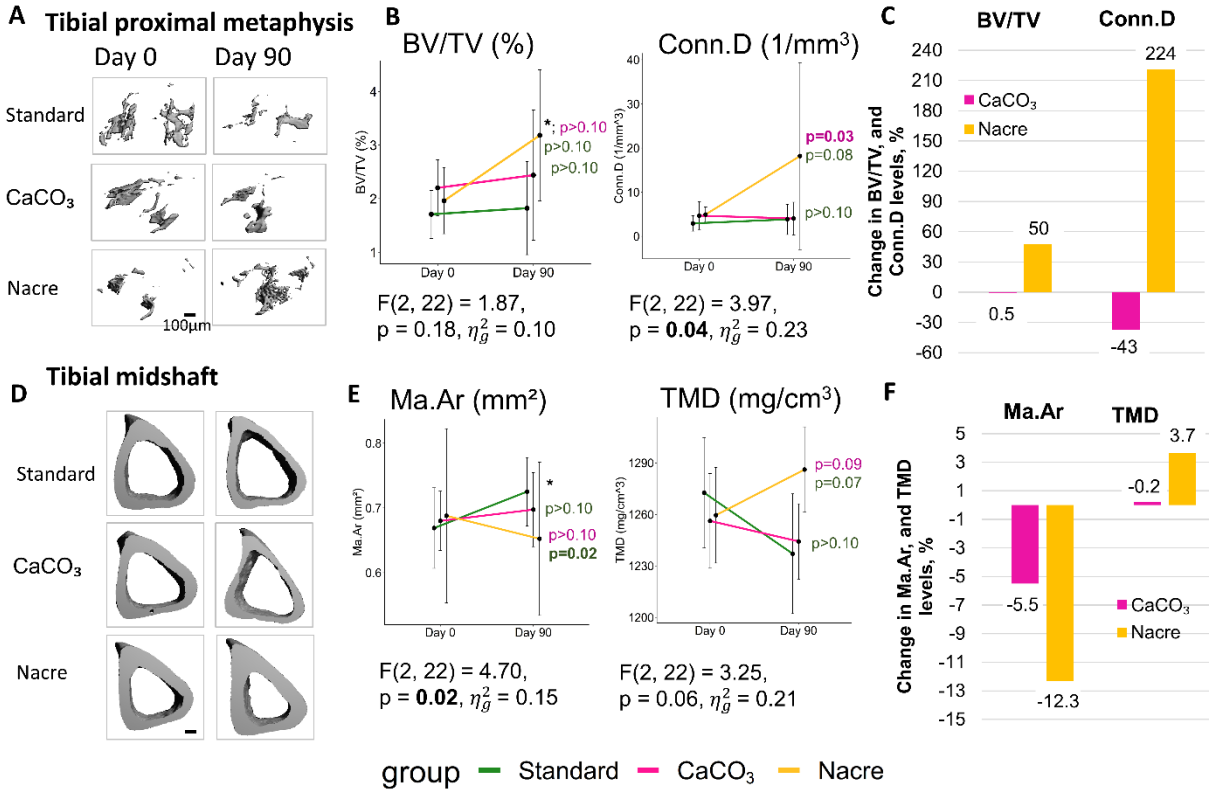

Fig. 2 Effect of nacre or calcium carbonate supplementation on cortical bone microarchitecture at the midshaft and the distal metaphysis of femur assessed by µCT (SkyScan) at the end of the study (day 90). (**A**) 3-dimensional (3D) reconstruction image of the whole femur, in which the top and bottom white lines depict the measured femoral length, and the dimensions of cortical and trabecular VOIs were analyzed (right pannel). (**B**) Representative coronal 2D images of full longitudinal femora of an animal (median BV/TV from each group). Scale bar, 1 mm. (**C**) Representative cortical bone 3D images at the femur midshaft and (**D**) the distal metaphysis. Scale bar, 500 µm. **(E-H**) Trabecular parameters at the distal metaphysis. **(I-K**) Cortical parameters at the distal metaphysis and the midshaft. * *vs*. distal metaphysis in each group; *p≤0.05, **p≤0.001, ***p≤0.0001. Data are represented as boxplots, and show all data points, with interquartile range (IQR) (height of the box), median (internal horizontal bar), and mean (black filled square, ▪). p-values in bold indicated statistical significance (p≤0.05). Standard: n=9, $CaCO_3$: n=11, Nacre: n=10.

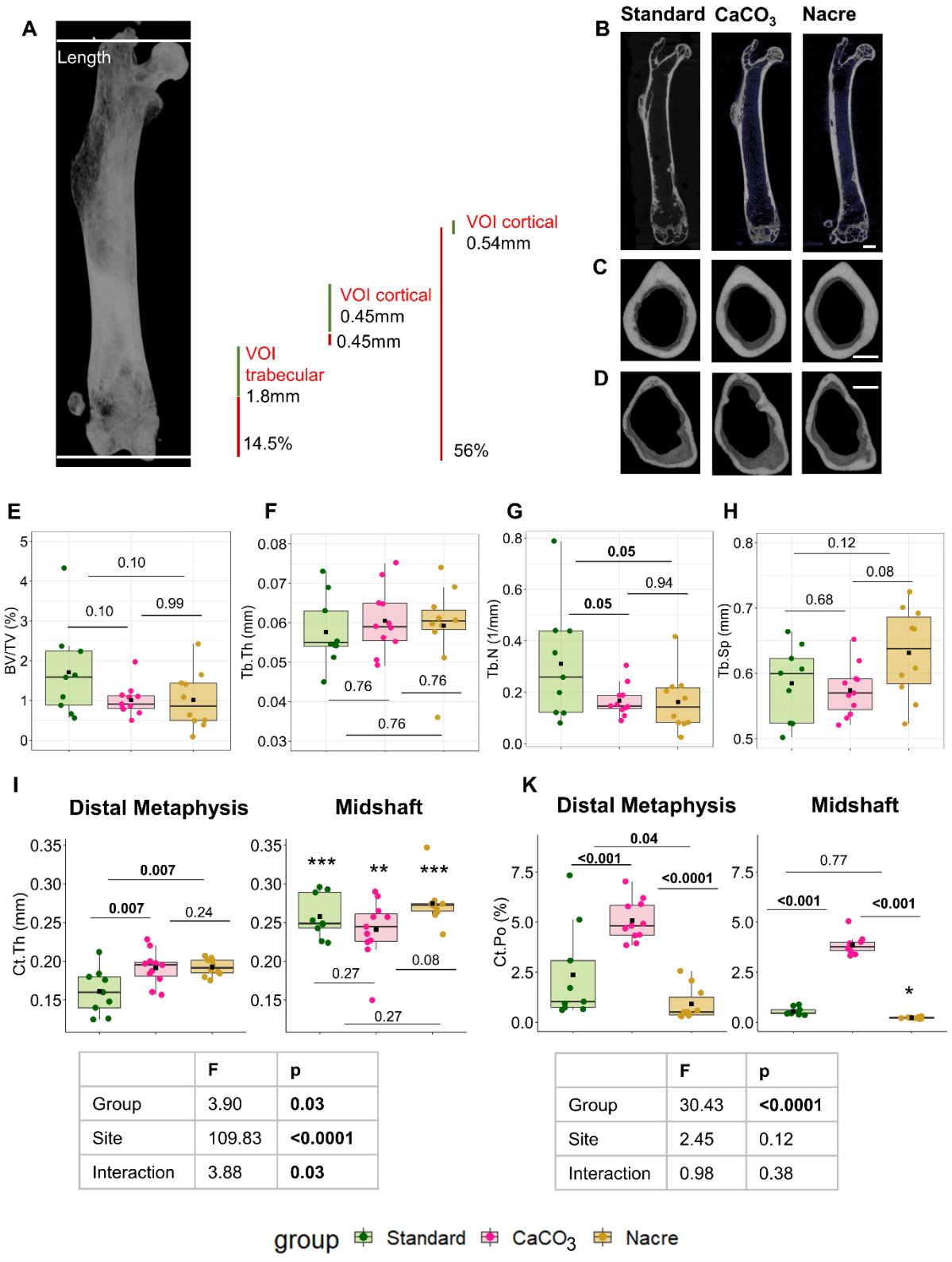

	F	p
Group	3.90	**0.03**
Site	109.83	**<0.0001**
Interaction	3.88	**0.03**

	F	p
Group	30.43	**<0.0001**
Site	2.45	0.12
Interaction	0.98	0.38

Fig. 3 Effect of nacre or calcium carbonate supplementation on mechanical properties of femora tested with three-point bending. (**A**) Representative load versus displacement curves for a triple of the heaviest (left graph) and lightest (right graph) mouse from each group (body weight indicated next to the curves in grams). Maximal force, Fmax (peak of the curve on the y-axis, black full circle •); Stiffness (slope of the linear portion of the curve, blue solid line); Breakage energy (area under the curve between Fmax point bordered with a black dashed line and zero point). (**B-D**) The raw parameters were derived from this test. (**E-G**) Same parameters as in B-D were adjusted for body weight. Data are represented as boxplots, and show all data points, with interquartile range (IQR) (height of the box), median (internal horizontal bar), and mean (black filled square, ▪). Standard: n=9, $CaCO_3$: n=11, Nacre: n=10. p-values in bold indicated statistical significance ($p \leq 0.05$). (**H, I**) Comparisons of linear regressions between Breakage energy and body weight for Standard versus Nacre and $CaCO_3$ versus Nacre.

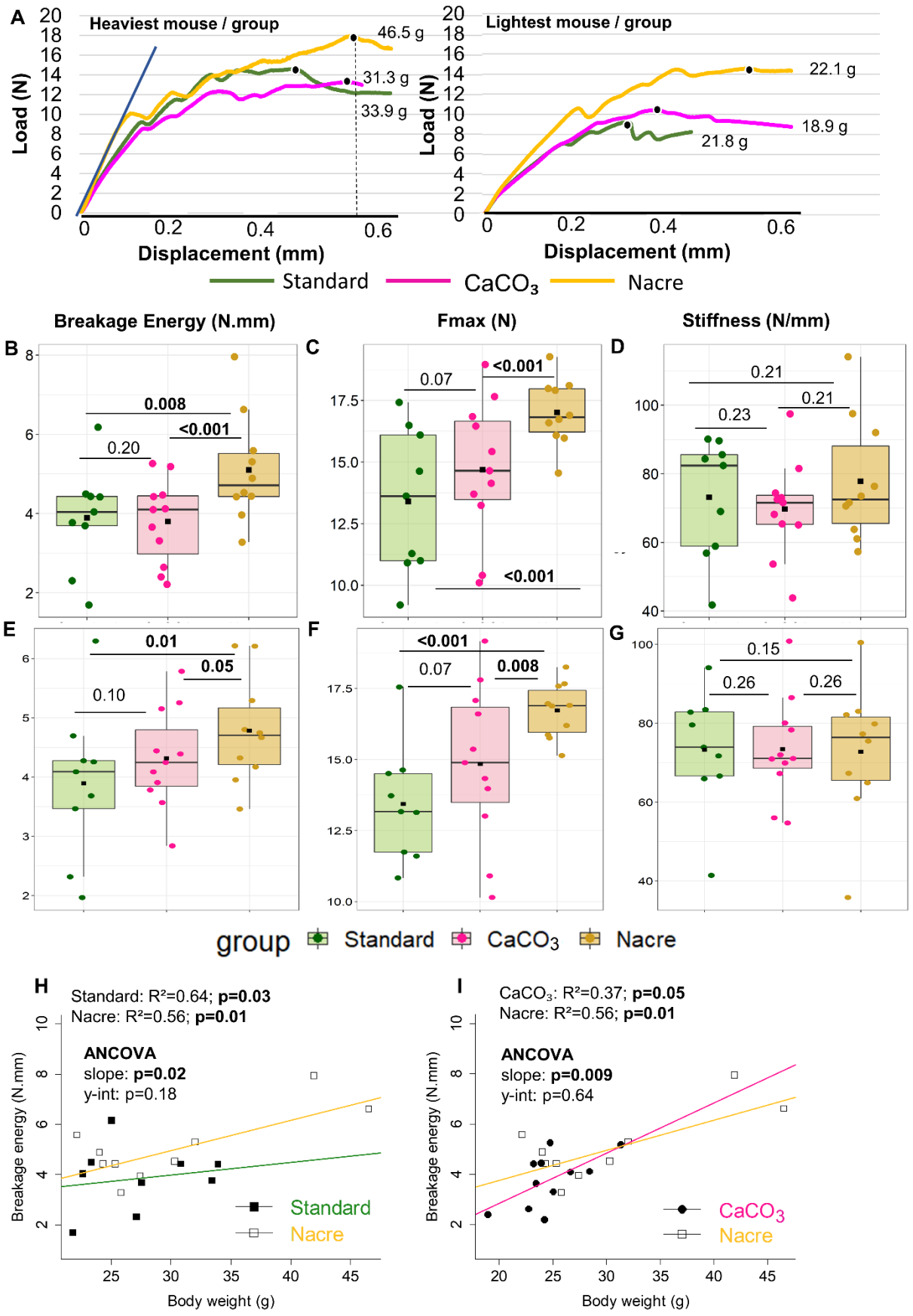
A
Heaviest mouse / group
46.5 g
31.3 g
33.9 g
Lightest mouse / group
22.1 g
18.9 g
21.8 g
Load (N)
Displacement (mm)
Standard
CaCO3
Nacre
Breakage Energy (N.mm)
Fmax (N)
Stiffness (N/mm)
B
C
D
E
F
G
0.008
<0.001
0.20
0.07
<0.001
<0.001
0.21
0.21
0.23
0.01
0.05
0.10
<0.001
0.07
0.008
0.15
0.26
0.26
group
Standard
CaCO3
Nacre
H
Standard: R²=0.64; p=0.03
Nacre: R²=0.56; p=0.01
ANCOVA
slope: p=0.02
y-int: p=0.18
I
CaCO3: R²=0.37; p=0.05
Nacre: R²=0.56; p=0.01
ANCOVA
slope: p=0.009
y-int: p=0.64
Breakage energy (N.mm)
Body weight (g)

Fig. 4 Effect of nacre or calcium carbonate supplementation on the distal femur trabecular bone histomorphometric parameters at day 90. (A) Osteoclast number per bone perimeter (N.Oc/B.Pm). **(B)** Osteoclast number per bone area (N.Oc/B.Ar). **(C)** Osteoclast surface per bone surface (Oc.S/BS). **(D)** Mineralizing surface per bone surface (MS/BS). **(E)** Mineral apposition rate (MAR). **(F)** Bone formation rate per bone surface (BFR/BS). Data are represented as boxplots, and show all data points, with interquartile range (IQR) (height of the box), median (internal horizontal bar), and mean (black filled square, ■). Sample sizes of static parameters: Standard: n=10, $CaCO_3$: n=9, Nacre: n=7; those of dynamic parameters: Standard or $CaCO_3$: n=3, Nacre: n=4. p-values in bold indicated statistical significance ($p \leq 0.05$).

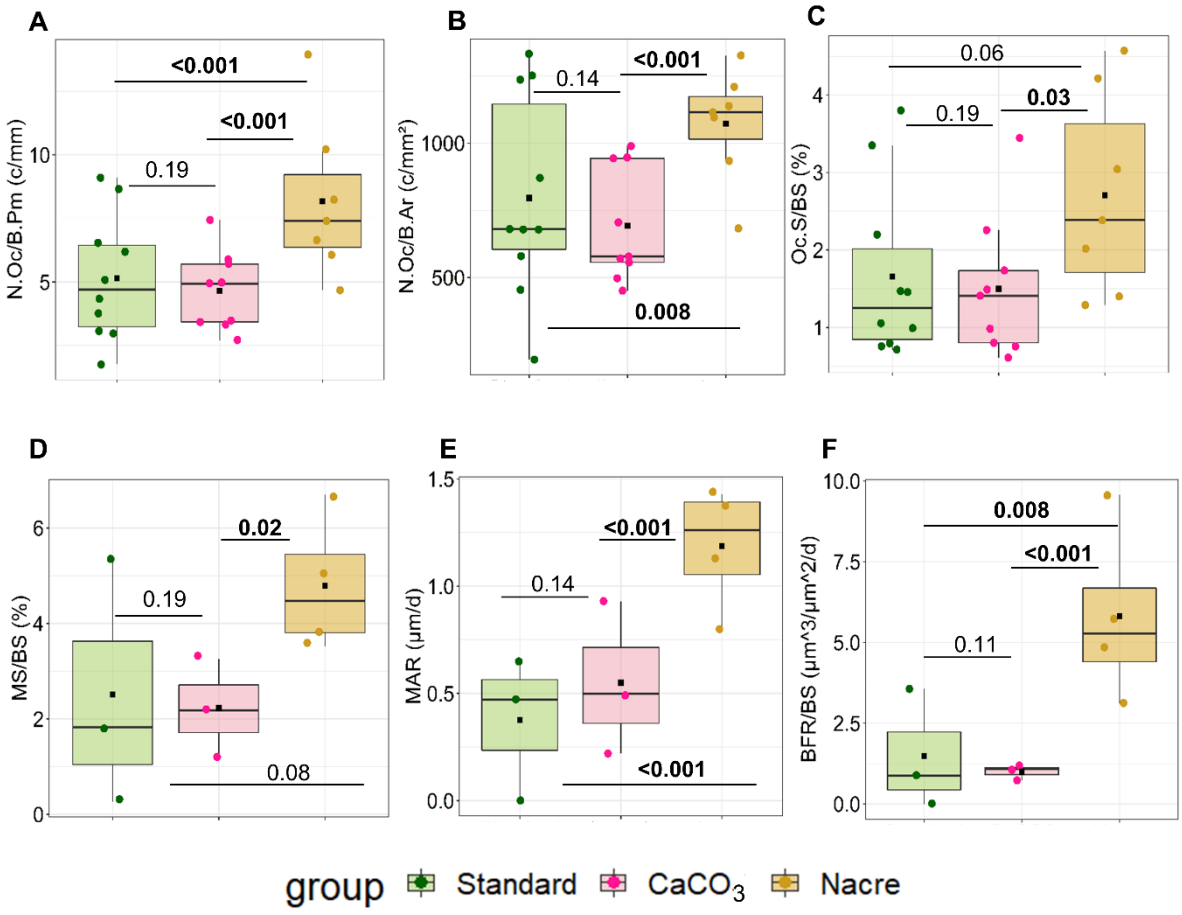

Fig. 5 Effect of nacre or calcium carbonate supplementation on mRNA expression levels in flushed bone marrow (A) and bone fraction (B) at day 90. Transcript levels are normalized to house-keeping gene *Hprt1* (hypoxanthine phosphoribosyltransferase 1). Data are represented as boxplots, and show all data points, with interquartile range (IQR) (height of the box), median (internal horizontal bar), and mean (black filled square, ■). Sample sizes of bone marrow: Standard or Nacre: n=7, $CaCO_3$: n=8; those of bone fraction: Standard: n=4, $CaCO_3$: n=6, Nacre: n=7. p-values in bold indicated statistical significance ($p \leq 0.05$).

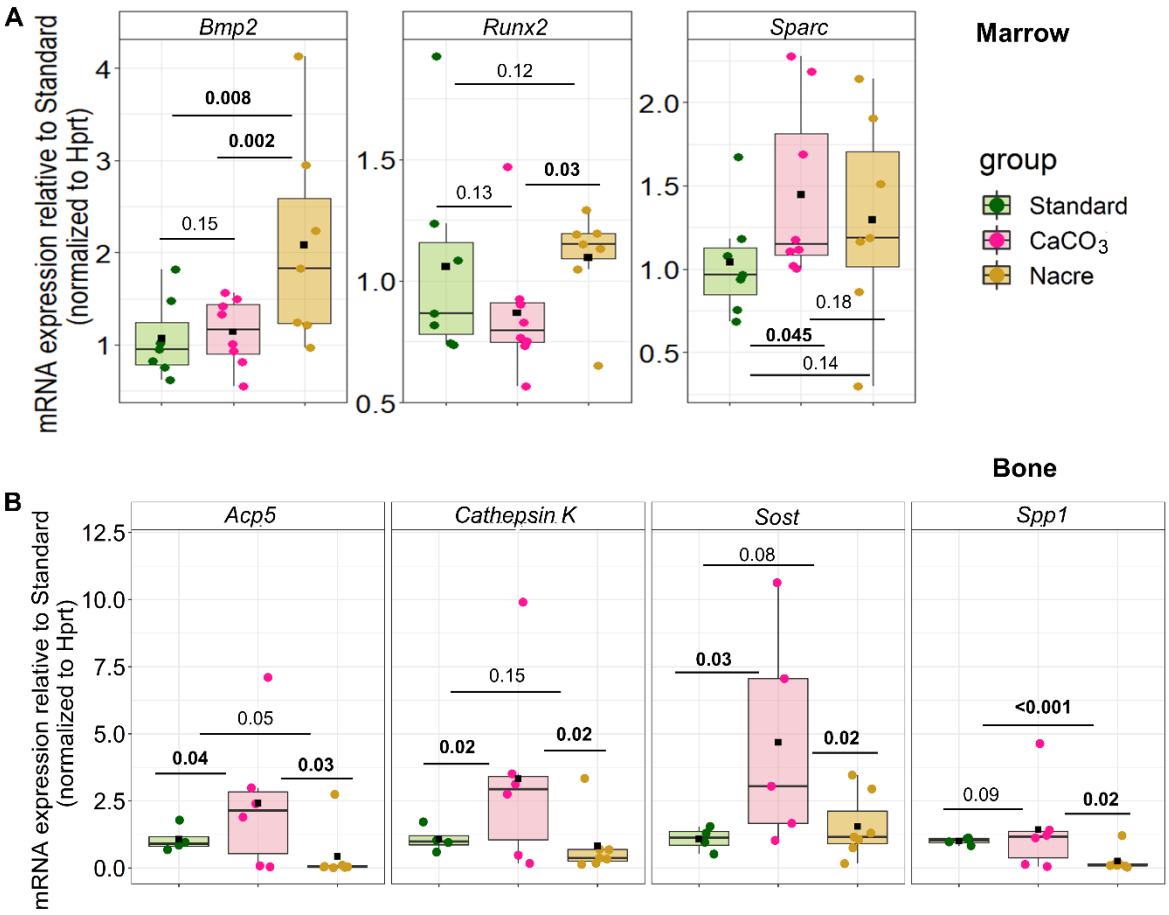

Fig. 6 Effect of nacre or calcium carbonate supplementation on serum bone turnover markers at day 0, 45 and 90 (A-C). Data are represented as the mean and sample distribution (Standard: n=8, $CaCO_3$: n=12, Nacre: n=11). [a] $p \leq 0.05$, [aa] $p \leq 0.01$, [aaa] $p \leq 0.001$, [a] *vs.* Standard; [*] *vs.* day 0, [#] *vs.* day 45. **(D-G) Serum levels of Calcium, Phosphate, FGF23, and PTH of these mice at day 90**. Data represent as boxplots, and show all data points, with interquartile range (IQR) (height of the box), median (internal horizontal bar), and mean (black filled square, ■). Standard: n=9, $CaCO_3$: n=12, Nacre: n=11. p-values in bold indicated statistical significance ($p<0.05$). The skewed raw data sets were transformed into a natural logarithm (Ln) to follow the normal distribution assumption.

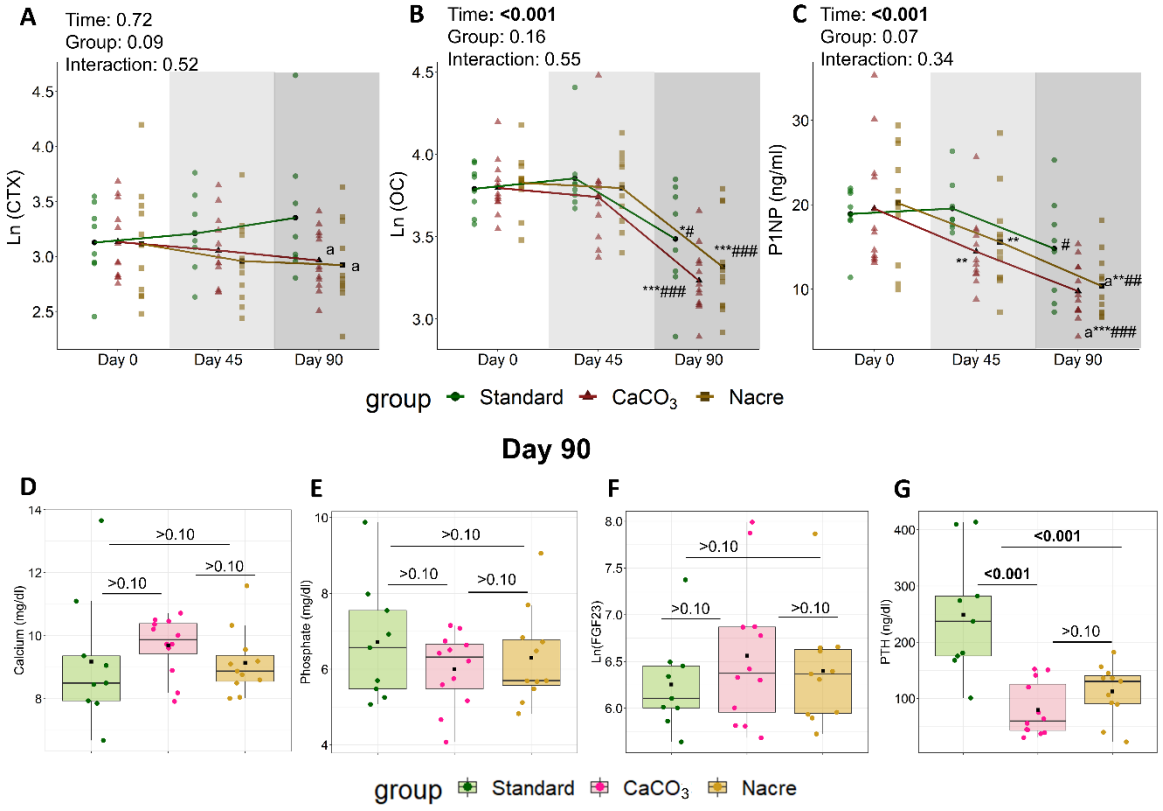

Tables

Table 1. Comparison of raw and body weight-adjusted values of cortical femur mechanical properties measured by three-point bending

(A) Standard (n=9; body weight = 27.3 (4.6) g) and $CaCO_3$ (n=11; body weight = 24.8 (3.2) g)						
Characteristic (unit)	Unadjusted			Body weight-adjusted		
	Standard	$CaCO_3$	95% CI †	Standard	$CaCO_3$	95% CI
Stiffness (N/mm)	73.2 (17.3) 24%	69.7 (13.9) 20%	-16.2 to 9.4	73.3 (14.9) 20%	73.4 (13.1) 18%	-10.7 to 13.3
Breakage energy (N.mm)	3.9 (1.3) 33%	3.8 (1.1) 28%	-1.1 to 0.9	3.9 (1.3) 33%	4.3 (0.8) 19%	-0.5 to 1.3
Fmax (N)	13.4 (2.9) 22%	14.7 (2.8) 19%	-0.9 to 3.4	13.4 (2.0) 15%	14.8 (2.8) 19%	-0.5 to 3.7
(B) Standard (n=9; body weight = 27.27 (4.57) g and Nacre (n=10; body weight = 29.96 (8.13) g)						
Characteristic (unit)	Unadjusted			Body weight-adjusted		
	Standard	Nacre	95% CI	Standard	Nacre	95% CI
Stiffness (N/mm)	73.2 (17.3) 24%	77.8 (18.0) 23%	-11.2 to 18.1	73.3 (14.9) 20%	74.9 (12.3) 16%	-11.2 to 10.3
Breakage energy (N.mm)	**3.9 (1.3)** **33%**	**5.1 (1.4)** **27%**	**0.2 to 2.5**	**3.9 (1.3)** **33%**	**4.8 (0.9)** **19%**	**0.1 to 1.9**
Fmax (N)	**13.4 (2.9)** **22%**	**17.0 (1.3)** **8%**	**1.8 to 5.4**	**13.4 (2.0)** **15%**	**16.7 (0.9)** **6%**	**2.1 to 4.6**
(C) $CaCO_3$ (n=11; body weight = 24.75 (3.22) g and Nacre (n=10; body weight = 29.96 (8.13) g)						
Characteristic (unit)	Unadjusted			Body weight-adjusted		
	$CaCO_3$	Nacre	95% CI	$CaCO_3$	Nacre	95% CI
Stiffness (N/mm)	69.7 (13.9) 20%	77.8 (18.0) 23%	-3.2 to 19.9	73.4 (13.1) 18%	74.9 (12.3) 16%	-10.7 to 13.3
Breakage energy (N.mm)	**3.8 (1.1)** **28%**	**5.1 (1.4)** **27%**	**0.3 to 2.3**	4.3 (0.8) 19%	4.8 (0.9) 19%	-0.1 to 1.3
Fmax (N)	**14.7 (2.8)** **19%**	**17.0 (1.3)** **8%**	**0.7 to 3.7**	**14.8 (2.8)** **19%**	**16.7 (0.9)** **6%**	**0.3 to 3.3**

Cortical femur properties were adjusted for body weight using the linear regression method according to the formula described in Method.
† Comparisons between groups were conducted by the Bootstrap method. 95% CI, 95% confidence interval
Values are mean (standard deviation, SD) and coefficient of variation, CV (%).
For ease of reading, the analysis results were presented in each pairwise comparison as in parts A, B, and C.
Bold values indicate statistically significant differences relative to the Standard (parts A, B) or $CaCO_3$ group (part C).